

# A new class of [2Fe-2S]-cluster-containing protoporphyrin (IX) ferrochelatases

Mark SHEPHERD, Tamara A. DAILEY and Harry A. DAILEY<sup>1</sup>

Biomedical and Health Sciences Institute, Paul D. Coverdell Center, University of Georgia, Athens, GA 30602, U.S.A.

Protoporphyrin (IX) ferrochelatase catalyses the insertion of ferrous iron into protoporphyrin IX to form haem. These ferrochelatases exist as monomers and dimers, both with and without [2Fe-2S] clusters. The motifs for [2Fe-2S] cluster co-ordination are varied, but in all cases previously reported, three of the four cysteine ligands are present in the 30 C-terminal residues and the fourth ligand is internal. In the present study, we demonstrate that a group of micro-organisms exist which possess protoporphyrin (IX) ferrochelatases containing [2Fe-2S] clusters that are co-ordinated by a group of four cysteine residues contained in an internal amino acid segment of approx. 20 residues in length. This suggests that these ferrochelatases have evolved along a different lineage than other bacterial protoporphyrin (IX) ferrochelatases.

For example, *Myxococcus xanthus* protoporphyrin (IX) ferrochelatase ligates a [2Fe-2S] cluster via cysteine residues present in an internal segment. Site-directed mutagenesis of this ferrochelatase demonstrates that changing one cysteine ligand into serine results in loss of the cluster, but unlike eukaryotic protoporphyrin (IX) ferrochelatases, this enzyme retains its activity. These data support a role for the [2Fe-2S] cluster in iron affinity, and strongly suggest convergent evolution of this feature in prokaryotes.

**Key words:** cluster, ferrochelatase, haem, iron–sulphur, mutagenesis, protoporphyrin IX.

## INTRODUCTION

Protoporphyrin (IX) ferrochelatase (protohaem ferro-lyase, EC 4.99.1.1) catalyses the insertion of a ferrous ion into the tetrapyrrole-derived ring of protoporphyrin IX, to yield protohaem and two protons [1,2]. A comparison of all currently known protoporphyrin (IX) ferrochelatases has revealed the presence of three distinct regions [2]. The first region (I) is present in all eukaryotes and has been identified as an N-terminal organelle targeting motif that is proteolytically cleaved following delivery to the organelle [3,4]. The second, (II), represents the core 330 amino acid residues and is ubiquitous amongst protoporphyrin (IX) ferrochelatases. The third region, (III), is a 30- to 50-amino acid C-terminal sequence that is found mainly in eukaryotic protoporphyrin (IX) ferrochelatases. Region III in animal protoporphyrin (IX) ferrochelatases is involved in dimerization of the enzyme [5], and contains three of the four cysteine ligands to an [2Fe-2S] cluster with the fourth being found in region II [5–8]. Region III of plant protoporphyrin (IX) ferrochelatase is approx. 50 residues and its role is currently unknown [2]. These ferrochelatases do not possess cysteine residues in region III and do not contain [2Fe-2S] clusters. Protoporphyrin (IX) ferrochelatase from the yeast, *Saccharomyces cerevisiae*, possesses a region III which lacks cysteine residues and does not contain an [2Fe-2S] cluster, whereas the *Schizosaccharomyces pombe* protoporphyrin (IX) ferrochelatase does possess the necessary cysteine residues and an [2Fe-2S] cluster [9].

The 2.0 Å (1 Å=0.1 nm) crystal structure of human protoporphyrin (IX) ferrochelatase has been solved using anomalous scattering signals generated from bound iron [5]. The asymmetric unit was found to contain a homodimer, with each monomer containing one [2Fe-2S] cluster. Each monomer contains two hydrophobic protrusions which flank the active site cleft and are proposed to be associated with the matrix side of the inner mitochondrial membrane. By contrast, the 1.9 Å crystal structure of *Bacillus subtilis* protoporphyrin (IX) ferrochelatase revealed a

soluble monomeric enzyme that lacks a [2Fe-2S] cluster [10]. More recently a small number of bacteria were identified that possess a C-terminal extension similar to that which is found in eukaryotic protoporphyrin (IX) ferrochelatases, and these also contain a [2Fe-2S] cluster [2,11]. In the present study, we report that yet another set of bacterial protoporphyrin (IX) ferrochelatases exist that possess a [2Fe-2S] cluster, but do not contain a C-terminal extension.

In the present study, we report steady-state kinetic characterization of this group of microbial protoporphyrin (IX) ferrochelatases. Genomic analysis demonstrates that a subset of these enzymes exists that co-ordinate [2Fe-2S] clusters, and that two distinct co-ordination motifs have evolved. Potential roles for the [2Fe-2S] cluster are presented and the evolutionary significance of these observations is discussed.

## EXPERIMENTAL

### Cloning and mutagenesis

*Mycobacterium tuberculosis* and *Caulobacter crescentus* protoporphyrin (IX) ferrochelatases were cloned and mutated as described previously [11]. Genomic DNA for *Pseudomonas aeruginosa* (a gift from Dr Wendy Dustman, Department of Microbiology, University of Georgia, Athens, GA, U.S.A.), *Porphyromonas gingivalis* (a gift from Dr James Travis, Department of Biochemistry and Molecular Biology, University of Georgia, Athens, GA, U.S.A.), and *Azotobacter vinelandii* (a gift from Dr William Lanzilotta, Department of Biochemistry and Molecular Biology, University of Georgia, Athens, GA, U.S.A.) was prepared [12]. Genomic DNA from *Myxococcus xanthus* was obtained from Dr Larry Shimkets (Department of Microbiology, University of Georgia, Athens, GA, U.S.A.). The genomic DNA of *Bdellovibrio bacteriovorus* was obtained from Dr John Iandolo (Department of Microbiology and Immunology, University of Oklahoma Health Sciences Center, Oklahoma City,

<sup>1</sup> To whom correspondence should be addressed (email hdailey@uga.edu).

OK, U.S.A.). *Pseudomonas putida* genomic DNA was purchased from American Type Culture Collection (A.T.C.C., Manassas, VA, U.S.A.). The cDNAs for *M. xanthus*, *A. vinelandii*, *P. putida*, *P. aeruginosa*, *P. gingivalis*, and *Bd. bacteriovorus* protoporphyrin (IX) ferrochelatases were amplified via PCR from genomic DNA using primers to introduce restriction sites for cloning into the expression vector pTrcHisA (Invitrogen), which contains an N-terminal His<sub>6</sub>-tag for ease of purification of the recombinant protein. Mutagenesis was performed using a QuikChange<sup>®</sup> kit (Stratagene), to create each of the *M. xanthus* (C213S, C219S, C220S, C230S and  $\Delta$ 209–230) and *P. putida* (D207C, K202T/D207C, K202T/ $\Delta$ V204/D207C and  $\Delta$ 202–225) mutants. The *Escherichia coli* *hemH* deletion mutant [13] was rendered chemically competent and transformed using each of the expression plasmids.

### Protein purification

Proteins were purified as described previously [11]. Yields of *M. xanthus* and *P. putida* protoporphyrin (IX) ferrochelatases were increased by including 1% Triton X-100 in the solubilization buffer. Protein concentration was determined using calculated extinction coefficients based on the amino acid sequence. These values were 48.8, 54.9, 53.5, 43.7, 43.0 mM<sup>-1</sup> · cm<sup>-1</sup> for *M. xanthus*, *P. putida*, *C. crescentus*, *M. tuberculosis* and *Bd. bacteriovorus* respectively.

### Spectroscopy

UV absorption spectra were measured with a Cary 50 spectrophotometer (Varian). Spectra were recorded in ferrochelatase solubilization buffer [50 mM Tris/Mops (pH 8.0), 100 mM KCl and 1.0% (w/v) sodium cholate].

### Substrate preparation

Mesoporphyrin IX (Porphyrin Products, Logan, UT, U.S.A.) was solubilized with a few drops of 30% NH<sub>4</sub>OH and then diluted with a 2% (v/v) solution of Triton X-100 immediately before use.

### Ferrochelatase assays

Iron chelation was measured using a continuous assay, by monitoring the depletion of mesoporphyrin IX absorbance at 496 nm using an extinction coefficient of 7.5 mM<sup>-1</sup> · cm<sup>-1</sup> [14]. This was performed using a Cary 50 spectrophotometer at 25 °C. The reactions were started by the addition of enzyme, which was pre-incubated at 25 °C, and the depletion of mesoporphyrin IX was monitored for 3 min. Where substrate inhibition was not present, fixed concentrations of 17  $\mu$ M mesoporphyrin IX and 50  $\mu$ M Fe<sup>2+</sup> were used when the other substrate was being varied. Where inhibition was observed at high concentrations of Fe<sup>2+</sup>, the ferrous iron concentration was fixed at 25  $\mu$ M when mesoporphyrin IX was varied. The concentration of iron was ranged from 5–50  $\mu$ M, and mesoporphyrin IX was ranged from 5–30  $\mu$ M. All assays contained 0.5  $\mu$ M protein, 50 mM Tris/MOPS (pH 8.0), 1% (v/v) Tween-20 and 5 mM 2-mercaptoethanol. The steady-state rates were estimated using linear regression of the time-course at the start of the reaction. *V* versus [S] curves were fitted to the Michaelis–Menten equation using non-linear regression (Sigmaplot 8).

## RESULTS

As part of an effort to elucidate the function of the [2Fe-2S] cluster in protoporphyrin (IX) ferrochelatases, our laboratory

performs sequence analysis of genomes as they become available in order to identify potential haem-synthetic enzymes. A TIGR (The Institute for Genome Research) BLAST screen using the genome of *M. xanthus* yielded a sequence in contig 581 which had reasonable similarity to known protoporphyrin (IX) ferrochelatase sequences. Pile-up analysis of this putative ferrochelatase sequence with several cluster containing protoporphyrin (IX) ferrochelatases, both eukaryotic and bacterial, revealed that the *M. xanthus* gene did not contain the required C-terminal extension found in protoporphyrin (IX) ferrochelatases that possess a [2Fe-2S] cluster. However, *M. xanthus* protoporphyrin (IX) ferrochelatase does possess a 22 amino acid insertion which contains four cysteine residues (Figure 1).

A BLAST search using the *M. xanthus* sequence yielded additional microbial protoporphyrin (IX) ferrochelatases with the insertion. Among these were *Bdellovibrio bacteriovorus*, *Pseudomonas syringae*, *Pseudomonas putida*, *Azotobacter vinelandii*, *Pseudomonas aeruginosa* and *Porphyromonas gingivalis*. Interestingly, three of these enzymes (from *A. vinelandii*, *Bdellovibrio bacteriovorus* and *P. syringae*) contained four cysteine residues in the insertion, whereas the other three contained one to three of the four cysteine residues (Figure 1).

### Mutagenesis

Recombinant protoporphyrin (IX) ferrochelatase from *M. xanthus*, *P. putida* and *P. aeruginosa* was expressed in *E. coli* and purified. UV spectra for these enzymes showed the presence of a [2Fe-2S] cluster in the *M. xanthus* enzyme but not in the *P. putida* or *P. aeruginosa* enzymes. The enzyme from *P. gingivalis* was expressed but precipitated immediately after purification, making it unsuitable for further analysis. The *A. vinelandii* enzyme was not expressed by this system.

To confirm that the four cysteine residues postulated as ligands to the [2Fe-2S] cluster are involved in cluster assembly, site-directed mutagenesis of the *M. xanthus* enzyme was performed to convert each individual cysteine residue (C213, C219, C220 and C230) into a serine residue. The absorption band at 330 nm and absorption peaks at approx. 415 and 550 nm that are characteristic of the [2Fe-2S] centre [8,15], are absent from the C213S, C219S (Figure 2, panel A), C220S and C230S spectra, indicating the loss of the cluster. Despite the absence of the cluster, each of these mutants was able to support the growth of the *E. coli*  $\Delta$ hemH strain [a strain lacking the *E. coli* protoporphyrin (IX) ferrochelatase enzyme]. Additional site-directed mutagenesis of the *M. xanthus* enzyme was performed to remove the cluster-ligating insertion. The resulting mutant,  $\Delta$ 209–230, retains enough activity to complement *E. coli*  $\Delta$ hemH, but was unstable after purification, preventing any biochemical analysis. The C219S mutant was selected for kinetic analysis, as described below.

The *P. putida* enzyme, which lacks a [2Fe-2S] cluster, contains three of the four cluster-ligating cysteine residues. In an attempt to create a [2Fe-2S] cluster in this enzyme, the amino acid in the position of the fourth cysteine ligand, which in *P. putida* is an aspartic acid, was mutated to cysteine. This recombinant enzyme (D207C) did not form a [2Fe-2S] cluster. To further mimic the sequence of the internal cluster-containing enzymes of *M. xanthus* and *A. vinelandii*, Lys<sup>202</sup> of the *P. putida* enzyme was mutated into a threonine residue in the previously mutated D207C enzyme. This enzyme (K202T/D207C) also did not form a [2Fe-2S] cluster. A third mutation, deletion of the valine residue at site 204 ( $\Delta$ V204/ K202T/D207C) to mimic the spacing of the *M. xanthus* enzyme, as well as the conserved residues at Lys<sup>202</sup> and Asp<sup>207</sup>, also did not assemble a cluster, suggesting that additional, currently unidentified residues spatially close to

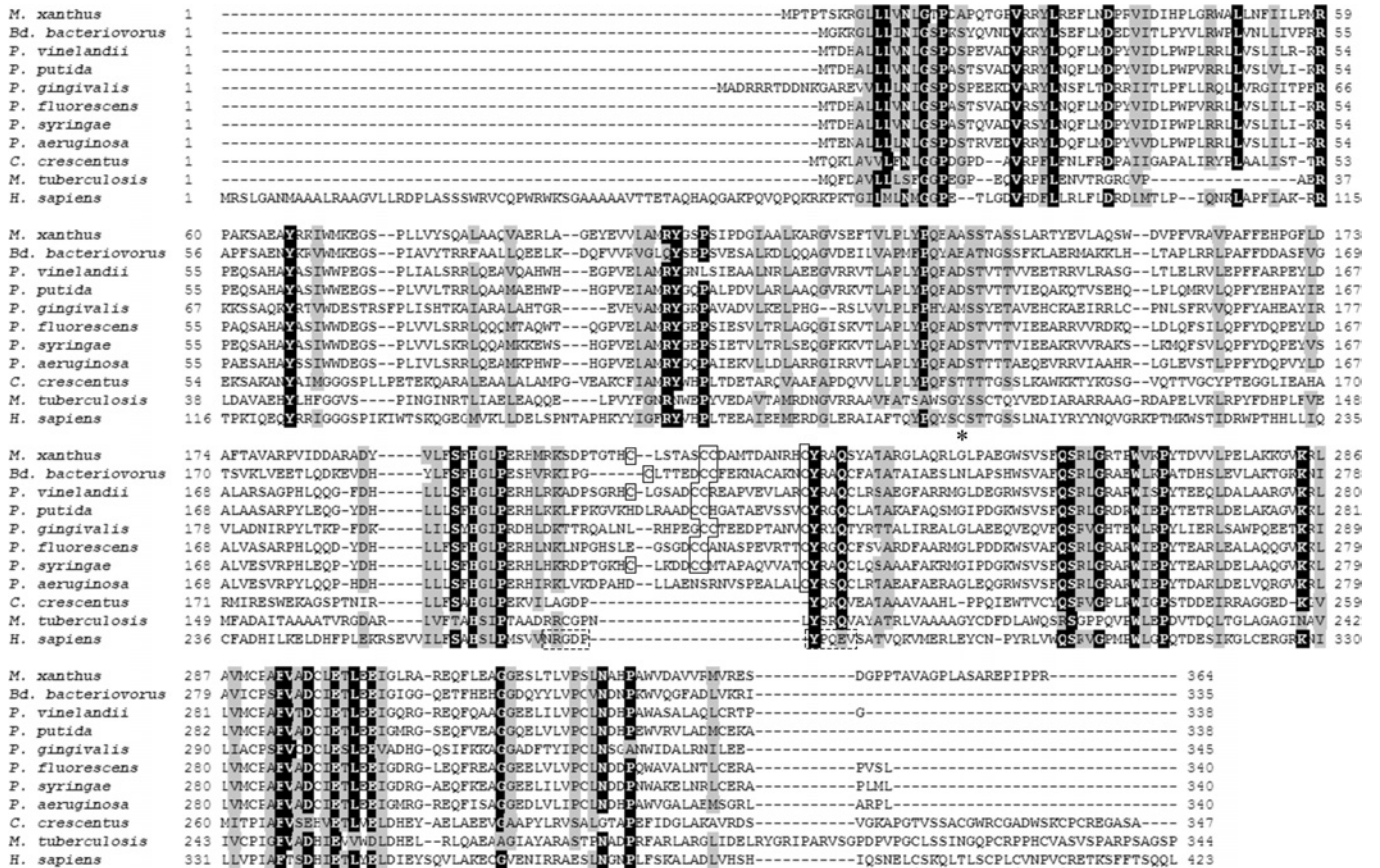


Figure 1 Multiple sequence alignment of protoporphyrin (IX) ferrochelatases

The black shading indicates a 90% sequence identity and the grey shading indicates where 90% of the residues are functionally similar. The solid boxes highlight potential conserved cysteine residues in the subset of ferrochelatases containing the 'cysteine-rich insertion'. \*, the cysteine ligands to the iron-sulphur cluster in human ferrochelatase. The broken-line boxes indicate the primary sequence of human ferrochelatase that is shaded in blue in Figure 5.

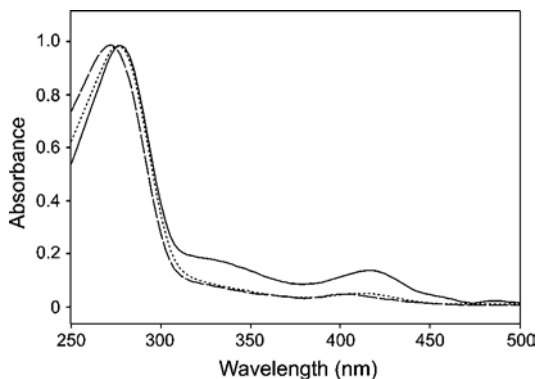


Figure 2 UV absorption spectra of protoporphyrin (IX) ferrochelatases

Absorption spectra of wild-type (solid line) and C219S mutant (dashed line) ferrochelatases from *M. xanthus*, and C341S mutant (dotted line) ferrochelatase from *C. crescentus*. The peak heights have been normalized for clarity.

the cluster are essential for assembly or stability. Deletion of the *P. putida* insertion resulted in an enzyme without the ability to rescue the growth of the *hemH* mutant of *E. coli*. This enzyme was not amenable to purification.

Protoporphyrin (IX) ferrochelatase from *C. crescentus*, which has previously been described [11], does not contain the cysteine-

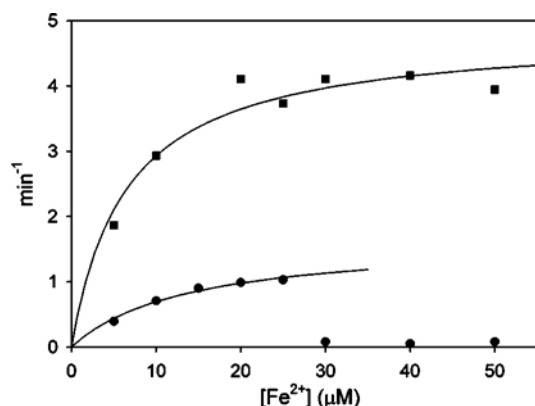
rich insert, but possesses a cysteine-rich C-terminal extension similar to that of the human enzyme (Figure 1). Attempts to produce a catalytically active *C. crescentus* enzyme that lacks the [2Fe-2S] cluster were made by mutating putative cluster-ligands into serine residues (C328S, C332S, C339S and C341S) [11]. In the current study the C341S enzyme was purified and subjected to kinetic characterization, as described below, to determine if the loss of the cluster elicited different effects compared with a protoporphyrin (IX) ferrochelatase that contains the cysteine-rich insert (*M. xanthus* C219S). The data shown in Figure 2 demonstrates that the C341S mutation results in the loss of the [2Fe-2S] cluster. The absorption spectrum of the *C. crescentus* wild-type enzyme resembles the *M. xanthus* wild-type spectrum shown in Figure 2, so was omitted for clarity.

Kinetic analysis

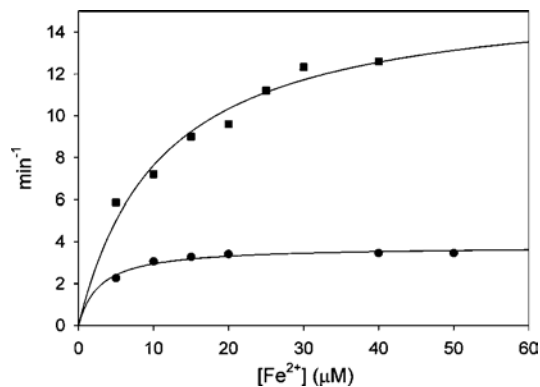
Wild-type protoporphyrin (IX) ferrochelatases from *M. xanthus*, *Bd. bacteriovorus*, *P. putida*, *M. tuberculosis* and *C. crescentus* were purified and subjected to preliminary kinetic analysis, along with two cluster-knockout mutant protoporphyrin (IX) ferrochelatases: *M. xanthus* C219S and *C. crescentus* C341S. Table 1 shows the kinetic parameters obtained when all of these purified enzymes were subjected to kinetic analysis. The data in Figure 3 shows the *V* versus [Fe<sup>2+</sup>] curves for *M. xanthus* wild-type and C219S mutant enzymes. Both are fitted to single rectangular

**Table 1** Kinetic parameters for various protoporphyrin (IX) ferrochelatases

Enzyme	Insertion	Cluster	$k_{cat}$ ( $\text{min}^{-1}$ )	$K_m^{\text{meso}}$ ( $\mu\text{M}$ )	$K_m^{\text{Fe}}$ ( $\mu\text{M}$ )
<i>M. xanthus</i> wild-type	Yes	Yes	$4.9 \pm 0.3$	$9.6 \pm 2.5$	$6.5 \pm 1.7$
<i>M. xanthus</i> C219S	Yes	No	$2.0 \pm 0.4$	$12.7 \pm 2.6$	$13.9 \pm 3.0$
<i>Bd. Bacteriovorus</i> wild-type	Yes	Yes	$4.4 \pm 0.3$	$8.0 \pm 2.1$	$28.0 \pm 2.9$
<i>P. putida</i> wild-type	Yes	No	$11.7 \pm 1.4$	$8.9 \pm 2.6$	$20.0 \pm 3.9$
<i>C. crescentus</i> wild-type	No	Yes	$16.0 \pm 1.2$	$8.7 \pm 2.3$	$11.0 \pm 2.3$
<i>C. crescentus</i> C341S	No	No	$3.8 \pm 0.1$	$4.7 \pm 1.0$	$2.8 \pm 0.5$

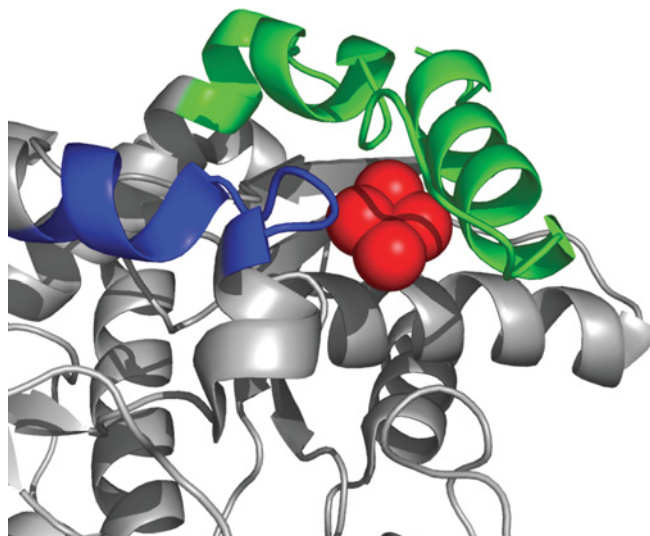
**Figure 3**  $V$  versus  $[\text{Fe}^{2+}]$  curves for *M. xanthus* wild-type (■) and C219S mutant (●) protoporphyrin (IX) ferrochelatases

Both datasets were fitted to single rectangular hyperbolae, but only the datapoints below  $25 \mu\text{M}$   $\text{Fe}^{2+}$  were used for the regression analysis of the C219S mutant data. The  $k_{cat}$  and  $K_{app}^{\text{Fe}}$  values for the wild-type enzyme were  $4.9 \pm 0.3 \text{ min}^{-1}$  and  $6.5 \pm 1.7 \mu\text{M}$  respectively. The  $k_{cat}$  and  $K_{app}^{\text{Fe}}$  values for the C219S mutant enzyme were  $2.0 \pm 0.4 \text{ min}^{-1}$  and  $13.9 \pm 3.0 \mu\text{M}$  respectively.

**Figure 4**  $V$  versus  $[\text{Fe}^{2+}]$  curves for *C. crescentus* wild-type (■) and C341S mutant (●) protoporphyrin (IX) ferrochelatases

Both datasets were fitted to single rectangular hyperbolae. The  $k_{cat}$  and  $K_{app}^{\text{Fe}}$  values for the wild-type enzyme were  $16.0 \pm 1.2 \text{ min}^{-1}$  and  $11.0 \pm 2.3 \mu\text{M}$  respectively. The  $k_{cat}$  and  $K_{app}^{\text{Fe}}$  values for the C431S mutant enzyme were  $3.8 \pm 0.1$  and  $2.8 \pm 0.5 \mu\text{M}$  respectively.

hyperbolae, although the data points above  $25 \mu\text{M}$   $\text{Fe}^{2+}$  for the mutant enzyme were omitted from the fitting. This *M. xanthus* C219S mutant enzyme is subject to iron substrate inhibition, and exhibits a larger  $K_m$  value for  $\text{Fe}^{2+}$  than the wild-type. Figure 4 shows the  $V$  versus  $[\text{Fe}^{2+}]$  curves for *C. crescentus* wild-type and C341S mutant enzymes. Both data-sets are fitted to single rectangular hyperbolae. The mutant enzyme appears to possess a lower  $K_m$  value for  $\text{Fe}^{2+}$  than that of the wild-type.

**Figure 5** Ribbon diagram of the human protoporphyrin (IX) ferrochelatase structure showing the spatial orientation of the  $[\text{2Fe-2S}]$  cluster and the cysteine residues co-ordinating it

The blue shading indicates the region of the human enzyme that corresponds to the cysteine rich insertion in some bacterial protoporphyrin (IX) ferrochelatases (broken-line box in Figure 1). The C-terminal extension found in human, but not these bacterial enzymes, is shown in green. The iron-sulphur cluster is shown in red.

## DISCUSSION

Above is reported the discovery of a new class of bacterial protoporphyrin (IX) ferrochelatases possessing internal insertions of approx. 20 amino acids, some of which contain a sufficient number of cysteine residues to ligate a  $[\text{2Fe-2S}]$  cluster. Among the enzymes containing the insertion, there are only six cysteine residues that are relatively conserved: the four within the insertion (in the enzymes which possess the four) and two additional cysteine residues at positions equivalent to human Pro<sup>334</sup> and His<sup>341</sup>, found in all of the insertion-containing enzymes. Since Pro<sup>334</sup> and His<sup>341</sup> residues are located in the active site spatially distant from any other cysteine residues, the cysteine residues occupying the analogous position in these bacterial ferrochelatases were not considered to be likely  $[\text{2Fe-2S}]$  cluster ligands. Site-directed mutagenesis of the four cysteine residues in the insertion in *M. xanthus* protoporphyrin (IX) ferrochelatase confirmed that the residues in the insertion were in fact responsible for co-ordination of the cluster.

Until the previous finding of  $[\text{2Fe-2S}]$  clusters in a limited number of bacterial protoporphyrin (IX) ferrochelatases [5], it was believed that this feature was restricted to higher animal protoporphyrin (IX) ferrochelatases. Although differences exist in the spacing between the three terminal cysteine residues, the general motif for cluster ligation found previously has been via four cysteines with one cysteine located near the middle of the primary sequence and the other three located within an approx. 30 residue C-terminal extension. By analogy with the human tertiary structure, it would be expected that this newly identified cluster resides in the same spatial location as does the  $[\text{2Fe-2S}]$  cluster in human protoporphyrin (IX) ferrochelatase (Figure 5). Although final determination of the exact orientation will require crystallographic data, it is highly unlikely that the spatial position will vary significantly, given the clear conservation of structure found between human [5], yeast [15a], and bacterial [10] protoporphyrin (IX) ferrochelatases reported to date.

The kinetic data obtained were for one bacterial C-terminal cluster-ligated protoporphyrin (IX) ferrochelatase: *C. crescentus*, and two internal insertion cluster-containing protoporphyrin (IX) ferrochelatases: *Bd. bacteriovorus* and *M. xanthus*. In addition, cluster-lacking C → S mutants for *C. crescentus* and *M. xanthus* were examined along with the *P. putida* wild-type enzyme, which has an internal insert, but lacks a [2Fe-2S] cluster. Although it was possible to produce and characterize stable mutant enzymes that lacked the normal [2Fe-2S] cluster (e.g. *M. xanthus* C219S and *C. crescentus* C341S), it has not yet proven possible to convert a non-cluster containing enzyme into a cluster-containing one. Attempts to convert the *P. putida* enzyme by introducing a fourth cysteine residue and changing the surrounding residues and spacing to resemble cluster-containing protoporphyrin (IX) ferrochelatases were unsuccessful. Interestingly, complete removal of the 22 amino acid residue insertion, which converts the protein into a more typical bacterial protoporphyrin (IX) ferrochelatase primary sequence, results in the production of an unstable protein.

Although it might be assumed that the variations in spacing of the terminal three cysteine residues found in previously reported bacterial protoporphyrin (IX) ferrochelatases arose through evolution by random mutagenesis of an ancestral cluster-containing bacterial ferrochelatase, the origin of the currently described clusters that are ligated by four cysteines in an internal insertion may best be attributed to convergent evolution. This fact makes clear the importance of the [2Fe-2S] cluster to the protoporphyrin (IX) ferrochelatases which possess it and argues that it is not just a randomly incorporated feature, but serves a significant *in vivo* function.

The kinetic data presented in Table 1 point to a potential difference in function between these two subsets of microbial ferrochelatases. The *M. xanthus* C219S mutant enzyme, which lacks the cluster, exhibits a larger apparent  $K_m$  value for iron than that of the wild-type enzyme, as well as being subject to inhibition by ferrous ion concentrations greater than 25  $\mu\text{M}$ . This suggests that the presence of the [2Fe-2S] cluster enhances iron binding at lower  $\text{Fe}^{2+}$  concentrations, and assists the productive binding at higher concentrations. Kinetic measurements were performed on two additional insert-containing protoporphyrin (IX) ferrochelatases from *Bd. bacteriovorus* and *P. putida*. The [2Fe-2S] cluster-containing *Bd. bacteriovorus* enzyme possesses a similar  $k_{\text{cat}}$  value to that of *M. xanthus* protoporphyrin (IX) ferrochelatase, although the  $K_m^{\text{Fe}}$  value is 4-fold larger than that of the *M. xanthus* enzyme. The cluster-less *P. putida* enzyme has a much larger  $k_{\text{cat}}$  value than the other members of this family possessing the [2Fe-2S] cluster. However, this enzyme only possesses three cysteine residues in the insert, and therefore does not co-ordinate a [2Fe-2S] cluster. The  $K_m^{\text{Fe}}$  of the *P. putida* enzyme is far higher than that of the *M. xanthus* wild-type enzyme. This is consistent with the theory that the [2Fe-2S] cluster enhances iron binding in this subset of protoporphyrin (IX) ferrochelatases. By contrast, the *C. crescentus* C341S mutant enzyme has a lower apparent  $K_m$  value for iron. This suggests that this cluster (not bound by an internal four cysteine insertion) may serve to down-regulate the incorporation of  $\text{Fe}^{2+}$  into protoporphyrin IX. Furthermore, the *C. crescentus* wild-type enzyme has a much larger  $k_{\text{cat}}$  value than protoporphyrin (IX) ferrochelatases containing the cysteine-rich insert, and removal of the cluster causes a 4-fold reduction in the  $k_{\text{cat}}$  value. However, removal of the cluster from the *M. xanthus* enzyme causes no significant decrease in the catalytic rate. Steady-state kinetic analysis was performed on the *M. tuberculosis* enzyme to support the data from the *C. crescentus* protoporphyrin (IX) ferrochelatase. However, this enzyme exhibits a much lower  $k_{\text{cat}}$  value compared with the wild-type *C. crescentus* enzyme, as

was previously described [11]. There are no data to explain this unusually low enzymatic activity.

Iron-sulphur clusters have been identified in other branches of tetrapyrrole metabolism. A 2Fe-2S centre has recently been shown to be present in sirohydrochlorin ferrochelatase from *Arabidopsis thaliana* (At-SirB) [16], whereas some cobaltochelates appear to harbour [4Fe-4S] centres [17]. The At-SirB sirohydrochlorin ferrochelatase was shown to contain a [2Fe-2S], which is proposed to be co-ordinated by three C-terminal cysteine residues and a conserved central cysteine residue, reminiscent of the mammalian protoporphyrin ferrochelatases. However, this ferrochelatase is very unstable and is degraded rapidly in an aerobic environment, unlike human protoporphyrin ferrochelatase, which gradually disappears over a period of 24 h [8]. The cobaltochelate, CbiX, is required for vitamin B<sub>12</sub> biosynthesis, and possesses a C-terminal MXCXC motif, which provides two of the four cysteine ligands to the [4Fe-4S] cluster [17]. Disruption of the Fe-S centre via mutagenesis of the cysteine ligands did not result in a reduction in catalysis. This observation is reminiscent of the results discussed in the present study, and could reflect another non-catalytic role for iron-sulphur clusters in ferrochelatases. Since the chelation rate was independent of the redox state of the cluster, the authors suggest that the redox centre does not act as a sensor, but may be present to interact with another protein, possibly involved in the delivery of cobalt to the active site. This is an interesting possibility, and is significant to the data in the present study, especially as loss of the cluster can have a significant effect on the  $K_m$  values for iron.

Since the clusters of the enzymes examined in the present study are not reduced by dithionite, it seems unlikely that the [2Fe-2S] cluster acts as a redox switch to modulate iron chelation. Furthermore, these clusters, unlike the eukaryotic protoporphyrin (IX) ferrochelatase [2Fe-2S] clusters, are very stable and are not destroyed by NO (T. A. Dailey, unpublished work). At present, there are no comprehensive studies published on the effect of cluster redox state on eukaryotic protoporphyrin (IX) ferrochelatase activity. However, given the differences in the physical properties of [2Fe-2S] clusters, it would not be unexpected if during evolution, a different role for the cluster in higher eukaryotes came into being. Indeed, the sensitivity of the animal cluster to NO results in diminished *in vivo* activity [18] and the lack of enzyme activity in the absence of the cluster means that cellular iron stores may influence the terminal step in haem biosynthesis [15]. Neither of these possibilities seem to be valid for bacterial systems. Nonetheless, it is clear that the presence of the [2Fe-2S] cluster in some bacterial protoporphyrin (IX) ferrochelatases creates ways in which cellular iron metabolism and/or other cellular/environmental factors can have an impact on haem synthesis. It is apparent that regulation of microbial iron and haem metabolism is complex and may be interrelated [20] and that the presence of the [2Fe-2S] cluster in some microbial protoporphyrin (IX) ferrochelatases may represent another piece of this puzzle of evolution.

This work was funded by the National Institutes of Health (grant DK32303 to H. A. D.).

## REFERENCES

- 1 Dailey, H. A. (1996) Ferrochelatase. In *Mechanisms of Metallocenter Assembly* (Hausinger, R. P., Einhorn, G. L. and Marzilli, L. G., eds.), pp. 77–98, VCH Inc., New York, U.S.A.
- 2 Dailey, H. A., Dailey, T. A., Wu, C. K., Medlock, A. E., Wang, K. F., Rose, J. P. and Wang, B. C. (2000) Ferrochelatase at the millennium: structures, mechanisms and 2Fe-2S clusters. *Cell. Mol. Life Sci.* **57**, 1909–1926
- 3 Karr, S. R. and Dailey, H. A. (1988) The synthesis of murine ferrochelatase *in vitro* and *in vivo*. *Biochem. J.* **254**, 799–803

- 4 Prasad, A. R. K. and Dailey, H. A. (1995) Effect of cellular location on the function of ferrochelatase. *J. Biol. Chem.* **270**, 18198–18200
- 5 Wu, C. K., Dailey, H. A., Rose, J. P., Burden, A., Sellers, V. M. and Wang, B. C. (2001) The 2.0 Å structure of human ferrochelatase, the terminal enzyme of heme biosynthesis. *Nat. Struct. Biol.* **8**, 156–160
- 6 Crouse, B. R., Sellers, V. M., Finnegan, M. G., Dailey, H. A. and Johnson, M. K. (1996) Site-directed mutagenesis and spectroscopic characterization of human ferrochelatase: identification of residues coordinating the 2Fe-2S cluster. *Biochemistry* **35**, 16222–16229
- 7 Sellers, V. M., Wang, K. F., Johnson, M. K. and Dailey, H. A. (1998) Evidence that the fourth ligand to the 2Fe-2S cluster in animal ferrochelatase is a cysteine – characterization of the enzyme from *Drosophila melanogaster*. *J. Biol. Chem.* **273**, 22311–22316
- 8 Dailey, H. A., Finnegan, M. G. and Johnson, M. K. (1994) Human ferrochelatase is an iron-sulfur protein. *Biochemistry* **33**, 403–407
- 9 Medlock, A. E. and Dailey, H. A. (2000) Examination of the activity of carboxyl-terminal chimeric constructs of human and yeast ferrochelatases. *Biochemistry* **39**, 7461–7467
- 10 Al Karadaghi, S., Hansson, M., Nikonov, S., Jonsson, B. and Hederstedt, L. (1997) Crystal structure of ferrochelatase: the terminal enzyme in heme biosynthesis. *Structure* **5**, 1501–1510
- 11 Dailey, T. A. and Dailey, H. A. (2002) Identification of 2Fe-2S clusters in microbial ferrochelatases. *J. Bacteriol.* **184**, 2460–2464
- 12 Wilson, K. (1994) Preparation of Genomic DNA from Bacteria. In *Current Protocols in Molecular Biology* (Ausubel, F. A., Kingston, R. E., Moore, D. D., Seidman, J. G., Smith, J. A. and Struhl, K., eds.), pp. 241–245, Greene Publishing and Wiley Interscience, New York, U.S.A.
- 13 Miyamoto, K., Nakahigashi, K., Nishimura, K. and Inokuchi, H. (1991) Isolation and characterization of visible light-sensitive mutants of *Escherichia-coli* K12. *J. Mol. Biol.* **219**, 393–398
- 14 Falk, J. E. (1964) *Porphyrins and metalloporphyrins: their general, physical and coordination chemistry, and laboratory methods*, Elsevier, Amsterdam, Netherlands
- 15 Sellers, V. M., Johnson, M. K. and Dailey, H. A. (1996) Function of the 2Fe-2S cluster in mammalian ferrochelatase: A possible role as a nitric oxide sensor. *Biochemistry* **35**, 2699–2704
- 15a Karlberg, T., Lecerof, D., Gora, M., Silvegren, G., Labbe-Bois, R., Hansson, M. and Al-Karadaghi, S. (2002) Metal binding to *Saccharomyces cerevisiae* ferrochelatase. *Biochemistry* **41**, 13499–13506
- 16 Raux-Deery, E., Leech, H. K., Nakrieko, K. A., McLean, K. J., Munro, A. W., Heathcote, P., Rigby, S. E. J., Smith, A. G. and Warren, M. J. (2005) Identification and characterization of the terminal enzyme of siroheme biosynthesis from *Arabidopsis thaliana* – a plastid-located siroheme chlorin ferrochelatase containing a 2Fe-2S center. *J. Biol. Chem.* **280**, 4713–4721
- 17 Leech, H. K., Raux, E., McLean, K. J., Munro, A. W., Robinson, N. J., Borrelly, G. P. M., Malten, M., Jahn, D., Rigby, S. E. J., Heathcote, P. and Warren, M. J. (2003) Characterization of the cobaltochelatase CbiX(L) – evidence for a 4Fe-4S center housed within an MXCXC motif. *J. Biol. Chem.* **278**, 41900–41907
- 18 Kim, Y. M., Bergonia, H. A., Muller, C., Pitt, B. R., Watkins, W. D. and Lancaster, J. R. (1995) Loss and degradation of enzyme-bound heme induced by cellular nitric-oxide synthesis. *J. Biol. Chem.* **270**, 5710–5713
- 19 Reference deleted
- 20 Qi, Z. H. and O'Brian, M. R. (2002) Interaction between the bacterial iron response regulator and ferrochelatase mediates genetic control of heme biosynthesis. *Mol. Cell* **9**, 155–162

Received 12 December 2005/8 March 2006; accepted 21 March 2006

Published as BJ Immediate Publication 21 March 2006, doi:10.1042/BJ20051967